Electronic Transitions in Doped and Undoped Copper Germanate

G. Yu. Rudko,[†] V. C. Long,[‡] and J. L. Musfeldt*[,§]

Department of Chemistry, State University of New York at Binghamton, Binghamton, New York 13902-6016

H.-J. Koo and M.-H. Whangbo

Department of Chemistry, North Carolina State University, Raleigh, North Carolina 27695-8204

A. Revcolevschi and G. Dhalenne

Laboratoire de Physicochimie des Solides, Université Paris−Sud, 91405 Orsay Cédex, France

D. E. Bernholdt

Computer Science and Mathematics Division, Oak Ridge National Laboratory, Oak Ridge, Tennessee 37831

Received August 31, 2000. Revised Manuscript Received January 8, 2001

We report an analysis of the absorption edge anisotropy in $CuGeO_3$ based on a comparison of polarized optical data with electronic structure calculations in the framework of the extended Hückel tight binding model. Taking the *z* axis as parallel to the CuO_4 chains, we ascribe the absorption edge in the magnetic chain direction to O $2p_x$, $2p_y \rightarrow$ singly filled Cu 3d transitions and the edge in the transverse direction to O $2p_z \rightarrow$ singly filled Cu 3d excitations. The dual slope in the transverse direction is a direct consequence of the double maximum in the O $2p_z$ density of states. The influence of Zn and Si doping on the electronic spectra of $CuGeO_3$ is analyzed as well. Whereas neither impurity affects the phonon-assisted d−d band, Si doping smears the charge-transfer gap. This smearing of the gap by interchain impurity substitution is attributed to random distortions of the crystalline lattice giving rise to structurally induced changes in the electronic properties.

I. Introduction

Both organic and inorganic spin-Peierls (SP) materials are of great interest because their investigation gives insight into the magnetic ordering of low-dimensional solids. At the same time, they exhibit rich phase diagrams and intriguing properties. Among these properties, two have attracted significant attention and seem to distinguish the inorganic materials. These include the tunability of spin exchange and superexchange interactions via doping without altering the overall crystallographic structure[1,2] and the coexistence of SP dimerization and Néel ordering[2−6] in the low-temperature region under appropriate doping conditions.

The SP transition has been observed in only a few inorganic crystals: $CuGeO_3$,[7] possibly $LiVGe_2O_6$,[8] and perhaps α'-NaV_2O_5 (in combination with charge ordering).[9] $CuGeO_3$ is the best studied of these systems. Its crystal lattice (space group *Pbmm*) is made up of distorted CuO_6 octahedra and GeO_4 tetrahedra. The CuO_6 octahedra share their trans edges to form CuO_4 chains running along the *c* axis. Likewise, the GeO_4 tetrahedra share their corners to form GeO_4 chains running along the *c* axis.[10,11] These chains are condensed such that each apical oxygen (O_{ap}) of a CuO_6 octahedron is shared by two GeO_4 tetrahedra and each basal oxygen of a CuO_6 octahedron with only one GeO_4 tetrahedron. A unit cell of $CuGeO_3$ has two CuO_4 chains,

* To whom correspondence should be addressed.
[†] Current address: Institute of Semiconductor Physics, National Academy of Sciences of Ukraine, Kiev-28, 252028 Ukraine.
[‡] Current address: Department of Physics and Astronomy, Colby College, Waterville, ME 04901.
[§] Current address: Department of Chemistry, University of Tennessee, Knoxville, TN 37996.

(1) Hase, M.; Terasaki, I.; Sasago, Y.; Uchinokura, K.; Obara, H. *Phys. Rev. Lett.* **1993**, *71*, 4059.
(2) Regnault, L. P.; Renard, J. P.; Dhalenne, G.; Revcolevschi, A. *Europhys. Lett.* **1995**, *32*, 579.
(3) Fronzes, P.; Poirier, M.; Revcolevschi, A.; Dhalenne, G. *Phys. Rev. B* **1997**, *55*, 8324.
(4) Kiryukhin, V.; Keimer, B.; Hill, J. P.; Coad, S. M.; Paul, D. McK. *Phys. Rev. B* **1996**, *54*, 7269.
(5) Sassago, Y.; Koide, N.; Uchinokura, K.; Martin, M. C.; Hase, M.; Hirota, K.; Shirane, G. *Phys. Rev. B* **1996**, *54*, R6835.
(6) Martin, M. C.; Hase, M.; Hirota, K.; Shirane, G.; Sasago, Y.; Koide, N.; Uchinokura, K. *Phys. Rev. B* **1997**, *56*, 3173.
(7) Hase, M.; Terasaki, I.; Uchinokura, K. *Phys. Rev. Lett.* **1993**, *70*, 3651.
(8) Millet, P.; Mila, F.; Zhang, F. C.; Mambrini, M.; Van Oosten, A. B.; Pashchenko, V. A.; Sulpice, A.; Stepanov, A. *Phys. Rev. Lett.* **1999**, *83*, 4176.
(9) Isobe, M.; Ueda, Y. *J. Phys. Soc. Jpn.* **1996**, *65*, 1178.
(10) Völlenkle, H.; Wittmann, A.; Nowotny, H. *Monatsh. Chem.* **1967**, *98*, 1352.
(11) Braden, M.; Wilkendorf, G.; Lorenzana, J.; M. Aïn, McIntyre, G. J.; Behruzi, M.; Heger, G. *Phys. Rev. B* **1996**, *54*, 1105.

10.1021/cm000703f CCC: $20.00
Published on Web 03/19/2001

and these two chains differ in the orientations of their edge-sharing planes. Note that the spin-$^1/_2$ Cu^{2+} chains are responsible for the magnetic properties of the material. At 14 K, $CuGeO_3$ undergoes a spin−lattice-driven dimerization to form the SP phase; the magnetic gap is 24 K.

In accordance with the quasi-one-dimensional structure of SP materials, there are two main ways to modulate the magnetic interactions. The first is to chemically substitute the magnetic species of the spin-$^1/_2$ chain with other cations that have a different value of spin. This kind of doping introduces interruptions into the chain, thus changing the magnetic interaction along the chain. A related modification is to substitute the nonmagnetic cations between the spin chains with other nonmagnetic ions, which changes the interchain interactions.

Pristine $CuGeO_3$ has been widely investigated by optical methods.[12−17] The main features of $CuGeO_3$ in the optical range are an anisotropic absorption edge (near 3 eV) due to charge-transfer transitions, a wide absorption band centered near 1.7 eV due to phonon-assisted d−d transitions that is largely responsible for the blue color of the crystals, and a tiny zero-phonon line on the low-energy side of the d−d band. Despite the doubling of the primitive cell and the related symmetry change at 14 K, the SP phase transition has little effect on the aforementioned optical properties. Only the zero-phonon line is sensitive to temperature and magnetic field transitions.[16,18] Spectroscopic studies of doped $CuGeO_3$ have been limited thus far to vibrational studies, searching for evidence of folded phonons, doping-induced modes, and magnetic field-induced modifications of the spin-gap excitation.[14,19−23] This presents an important opportunity for further investigation.

To probe the nature of the absorption edge anisotropy and the phonon-assisted d−d transitions in $CuGeO_3$-based materials, we have measured the polarized transmittance spectra of pristine and doped crystals. We combine our analysis of the experimental spectra with density of states calculations and group theory considerations. We also seek to understand how intra- and interchain doping affect the color properties in this family of compounds and to analyze possible mechanisms of this influence.

Table 1. Exponents ζ_i and the Valence Shell Ionization Potentials H_{ii} of Slater-Type Orbitals χ_i Used for Extended Hückel Tight-Binding Calculation[a]

atom	c_i	H_{ii} (eV)	ζ_i	c_1[b]	ζ_i	c_2[b]
Cu	4s	−11.4	2.151	1.0		
Cu	4p	−6.06	1.370	1.0		
Cu	3d	−14.0	7.025	0.4473	3.004	0.6978
Ge	4s	−9.00	2.160	1.0		
Ge	4p	−6.06	1.850	1.0		
O	2s	−32.3	2.275	1.0		
O	2p	−14.8	2.275	1.0		

[a] H_{ii}'s are the diagonal matrix elements $\langle\chi_i|H^{\text{eff}}|\chi^i\rangle$, where H^{eff} is the effective Hamiltonian. In our calculations of the off-diagonal matrix elements $H^{\text{eff}} = \langle\chi_i|H^{\text{eff}}|\chi^i\rangle$, the weighted formula was used. See ref 38. [b] Coefficients used in the double-ζ Slater-type orbital expansion.

II. Methods

Single crystals of pure and doped $CuGeO_3$ were grown by floating zone techniques using an image furnace.[24] According to ICP/AES measurements, the impurity concentrations were 0.7, 1.5, and 4.0% for Zn and 0.7% for Si. Samples for transmission measurements were cleaved from the original single crystals along the *bc* plane with thicknesses between 30 and 40 μm, measured to an accuracy of ±15%.[25]

The polarized optical transmittance was measured in the spectral range from 300 to 3000 nm (≈0.4−4.1 eV) using a modified Perkin-Elmer Lambda-900 spectrometer. The resolution was 2 and 5 nm in the UV/visible and near-infrared ranges, respectively. The polarization was chosen in accordance with the largest spectral anisotropy at room temperature, corresponding to the *b* and *c* axes, respectively. An open-flow cryostat system was used for variable-temperature experiments. Absorption ($\alpha(\omega)$) was calculated from the measured transmittance, taking into account the sample thickness and average reflectance.[25,26]

Standard PeakFit procedures were used to fit the complex color band absorption centered near 1.7 eV. A variety of line shapes were tested for suitability, including Lorentzian, Voigt, asymmetric double Gaussian cumulative, and asymmetric double sigmoid. Overall, a Gaussian shape gave the most satisfactory results for the three oscillators of the color band. Errors were estimated statistically, based upon the results obtained for slightly different fitting procedures involving variable background choices.

Electronic structure calculations were carried out for $CuGeO_3$ using the extended Hückel tight binding method.[27−31] To help interpret our optical data, electronic structure calculations were also carried out for an isolated CuO_4 chain and an isolated CuO_6 octahedron. For our discussion of the electronic structures of $CuGeO_3$ and the isolated CuO_4 chain, we choose the local Cartesian coordinates such that the *z* axis runs along the CuO_4 chain direction. Table 1 summarizes the parameters of the atomic orbitals used in our extended Hückel electronic structure calculation.

(12) Terasaki, I.; Itti, R.; Koshizuka, N.; Hase, M.; Tsukuda, I.; Uchinokura, K. *Phys. Rev. B* **1995**, *52*, 295.
(13) Bassi, M.; Camagni, P.; Rolli, R.; Samoggia, G.; Parmigiani, F.; Dhalenne, G.; Revcolevschi, A. *Phys. Rev. B* **1996**, *54*, R11030.
(14) Damascelli, A.; van der Marel, D.; Dhalenne, G.; Revcolevschi, A. *Phys. Rev. B* **2000**, *61*, 12063.
(15) Dević, S. D.; Popović, Z. V.; Breitschwerdt, A.; Dhalenne, G.; Revcolevschi, A. *Phys. Status Solidi B* **1997**, *203*, 579.
(16) Long, V. C.; Musfeldt, J. L.; Schmiedel, T.; Revcolevschi, A.; Dhalenne, G. *Phys. Rev. B* **1997**, *56*, 14263.
(17) Popova, M. N.; Sushkov, A. B.; Golubchik, S. A.; Vasil'ev, A. N.; Leonyuk, L. I. *Phys. Rev. B* **1998**, *57*, 5040.
(18) Zeman, J.; Martinez, G.; van Loodsdrecht, P. H. M.; Dhalenne, G.; Revcolevschi, A. *Phys. Rev. B* **1999**, *83*, 2648.
(19) Weiden, M.; Hauptmann, R.; Richter, W.; Köppen, M.; Steglich, F.; Fischer, M.; Lemmens, P.; Güntherodt, G.; Krimmel, A.; Nieva, G. *Phys. Rev. B* **1997**, *55*, 15067.
(20) Jandl, S.; Poirier, M.; Castonguay, M.; Fronzes, P.; Musfeldt, J. L.; Revcolevschi, A.; Dhalenne, G. *Phys. Rev. B* **1996**, *54*, 7318.
(21) Sekine, T.; Kuroe, H.; Sasaki, J.; Uchinokura, K.; Hase, M. *J. Magn. Magn. Mater.* **1998**, *177−181*, 691.
(22) McGuire, J. J.; Rõõm, T.; Mason, T. E.; Timusk, T.; Dabkowska, H.; Coad, S. M.; Paul, D. Mck. *Phys. Rev. B* **1999**, *59*, 1157.
(23) Jones, B. R.; Sushkov, A. B.; Musfeldt, J. L.; Wang, Y. J.; Revcolevschi, A.; Dhalenne, G. *Phys. Rev. B*, in press.
(24) Revcolevschi, A.; Collongues, R. *C. R. Acad. Sci.* **1969**, *266*, 1767.
(25) Sample thickness determination is the primary source of error in the calculated absorption values. We estimate that that thickness is known to an accuracy of ±15%.
(26) Another source of uncertainty in the determination of the absolute absorption level is the magnitude of reflectance. On the basis of a number of considerations for our samples, we selected an average optical reflectance of 0.06 and used this value for all of the impurity-substituted samples studied here. This differs from the values of 0.13[18] and 0.16/0.18[13,17] used in the previous work.
(27) Hoffmann, R. *J. Chem. Phys.* **1963**, *39*, 1397.
(28) Whangbo, M.-H.; Hoffmann, R. *J. Am. Chem. Soc.* **1978**, *100*, 6397.
(29) Our calculations were carried out using the CAESAR program package (Ren, J.; Liang, W.; Whangbo, M.-H. *Crystal and Electronic Structure Analysis Using CAESAR*, 1998. This book can be downloaded free of charge from the web site http://www.PrimeC.com/).
(30) Canadell, E.; Whangbo, M. H. *Chem. Rev.* **1991**, *91*, 965.
(31) Whangbo, M.-H. *Theor. Chem. Acc.* **2000**, *103*, 252.

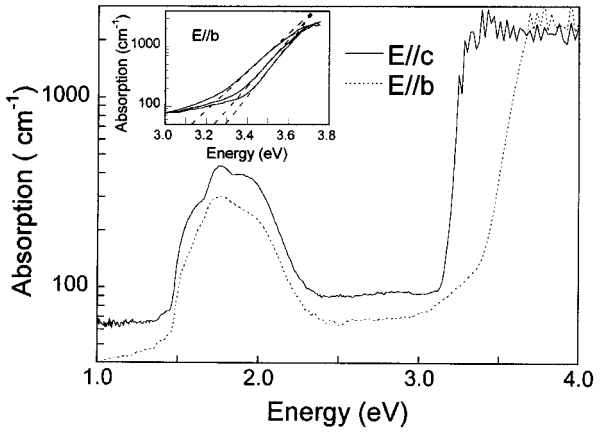

Figure 1. Polarized optical absorption of $CuGeO_3$ at $T = 10$ K. Solid line: $E\|c$. Dashed line: $E\|b$. Inset: absorption spectra of $CuGeO_3$ in $E\|b$ polarization at different temperatures (solid curves) and linear fits to these curves (dashed lines) in accordance with the Urbach rule. From left to right: 70, 180, and 300 K.

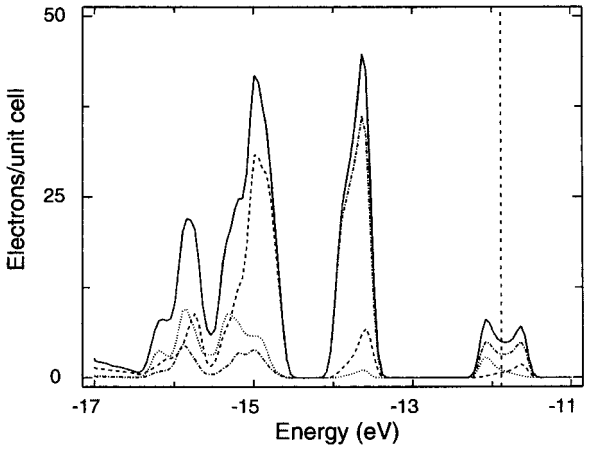

Figure 2. Calculated densities of state for the d-block bands of $CuGeO_3$. Solid curve: total densities of state. Dotted line: p_z states of basal oxygen atoms. Dashed line: $p_x + p_y$ states of basal oxygen atoms. Dash-dotted line: Cu 3d states. Note that the z axis is taken along the CuO_4 chain direction.

III. Results and Discussion

A. Anisotropy of the Electronic Gap Excitation in Pristine $CuGeO_3$. Figure 1 displays the absorption spectra of undoped $CuGeO_3$ in the *b*- and *c*-axis polarizations at ≈10 K. The spectra exhibit a strongly anisotropic absorption edge above 3 eV and a more complex band centered near 1.7 eV, with comparatively low absorption, in excellent agreement with previous optical investigations.[13−17] These spectral features have been widely discussed in the past. The optical gap near 3 eV was originally ascribed to a d−d or interband transition,[12,17] but more recent work[13,14,32] interprets it in terms of O → Cu charge-transfer excitations. In addition to the aforementioned gap edge anisotropy, the spectrum transverse to the magnetic chain displays a more complicated shape, evidence of multiple excitations contributing to the character of the gap edge. The 1.7 eV absorption band is attributed to localized dipole-forbidden transitions between the Cu^{2+} d states which become allowed via phonon assistance. Participation of phonons in this absorption process was shown explicitly by an analysis of the temperature dependence of the d-band oscillator strength, showing a coth($h\nu/kT$) response.[13,17] Note that, apart from the tiny zero-phonon line at 1.47 eV,[16,18] there are no electronic structure changes on passing through the spin-Peierls transition.

The absorption edge of $CuGeO_3$ was previously analyzed in terms of direct band-to-band transitions[15] and using the empirical Urbach rule,[13,33] where the absorption threshold at various temperatures is fit by an exponential dependence of frequency and reciprocal temperature. We have applied several kinds of treatment to our experimental absorption data, fitting the spectra to both direct and indirect band-to-band models as well as the phenomenological Urbach rule.[33] We find that the Urbach rule reasonably describes the $E\|c$ absorption edge over a wide range of absorption values. As seen from the inset to Figure 1, however, Urbach fitting of $E\|b$ data is less conclusive, even at low temperature. Whereas Urbach straight lines exhibit fairly good agreement with the spectra at absorption values larger than 100 cm^{-1}, another less abrupt slope is clearly observed in the spectra at lower absorption levels. A plot of $\sqrt{\alpha(\omega)}$ vs E also gives two slopes, resembling indirect behavior. (Here, $\alpha(\omega)$ is the frequency-dependent absorption, and E is the energy.) One might ascribe the second slope to phonon participation in the transition. Estimating the phonon energy from the intersection of this inclined line with the energy axis, we extract a value of ≈1500 cm^{-1}, which is much too large to be a phonon in the $CuGeO_3$ system. This leads to an impasse in the analysis and makes interpretation within both Urbach and valence/conduction band models less attractive for explaining the subtleties in this system. Clearly, the unusual shape of the edge in the *b* direction is not the result of an isolated excitation. To understand the origin of this ubiquitous "second slope" in the $E\|b$ absorption data near the optical gap (observed in all samples investigated here as well as in earlier studies of the pristine material), we examined the calculated electronic structure for $CuGeO_3$ and a single CuO_4 chain.

Figure 2 displays the total (solid line) and partial (broken lines) densities of state calculated for $CuGeO_3$. Only the energy region of the d-block bands is presented for simplicity. The total densities of state plot for the d-block bands calculated in the present work is quite similar in general feature to that reported by Mattheiss from first-principles electronic band structure calculations.[34] The $p_{x,y,z}$ states of oxygen (with a small admixture of d states of Cu) form the wide band in the energy region from −16.5 to −14.5 eV. To discuss the orbital character of the d-block bands (the peaks around −13.7 and −12.0 eV), it is convenient to employ the same local coordinate system as that used for the electronic structure calculations. The ordering of the 3d levels of an isolated CuO_6 octahedron shown in the inset of Figure 4 is thus based on the choice of the coordinate system in which the z axis runs along the CuO_4 chain direction and the basal plane of the CuO_6 octahedron lies in the xz plane. In this coordinate system, the d_{xz} level becomes

(32) Parmigiani, F. *Phys. Rev. B* **1997**, *55*, 1459.
(33) Urbach, F. *Phys. Rev.* **1953**, *92*, 1324.
(34) Mattheiss, L. F. *Phys. Rev. B* **1994**, *49*, 14050.

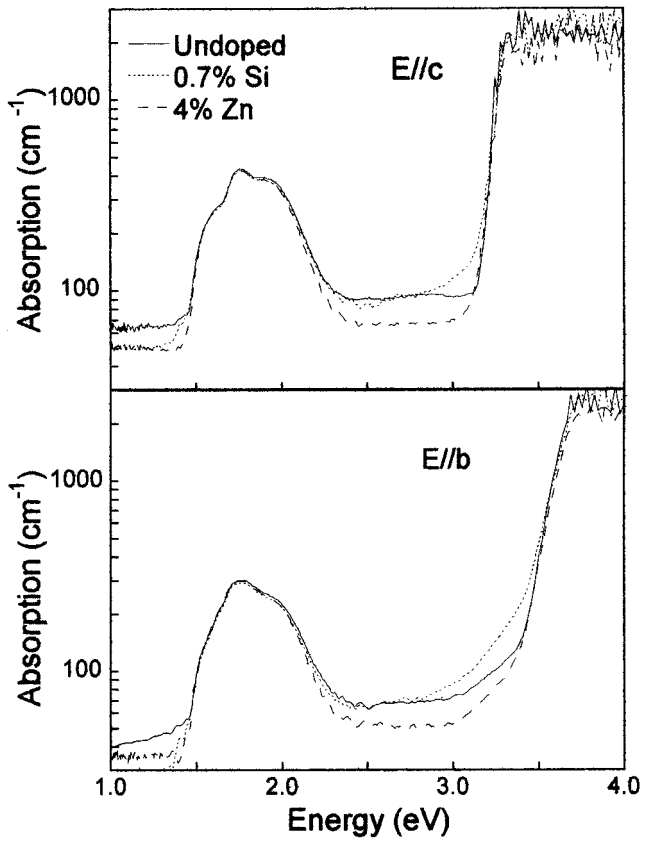

Figure 3. Absorption spectra of pure and doped $CuGeO_3$ in *E*||*c* (upper panel) and *E*||*b* (lower panel) polarizations. Solid line: pristine $CuGeO_3$. Dotted line: 0.7% Si doping. Dashed line: 4% Zn doping. The spectra are taken at ≈10 K.

the highest occupied 3d level and is half-filled. (With a conventional choice of the coordinate system in which the *x* and *y* axes are taken along the Cu−O bonds of the basal plane, the $d_{x^2-y^2}$ level is the singly filled 3d level of the CuO_6 octahedron.) In Figure 2, the narrower structure centered near −13.7 eV is formed predominately by doubly filled 3d levels of the CuO_6 octahedra, and the feature near −12 eV results largely from singly filled 3d levels of the CuO_6 octahedra. The latter band is half-filled, so that in a hypothetical, metallic state of $CuGeO_3$ the Fermi level would be located in the middle of this band, as shown in Figure 2. However, the magnetic insulating state of the CuO_4 chain should be represented by the band filling in which all levels of this band are singly occupied.[31,35] The Fermi level corresponding to a metallic state is shown for the magnetic insulating state simply to indicate which band is half-filled. Although off the scale of Figure 2, the densities of state calculated for $CuGeO_3$ has additional maxima near −5.5 and −1.5 eV, which are related to the s and p states of both Cu and Ge. The assignment of the p_x and p_y bands in the partial densities of state (PDOS) of $CuGeO_3$ was verified by analogous calculations for an isolated CuO_4 chain. As expected, the essential features of the electronic structure of $CuGeO_3$ presented in Figure 2 are also found in the electronic structure calculated for an isolated CuO_4 chain (not shown). The advantage is that, in the latter case, PDOS curves for

(35) Whangbo, M.-H. *J. Chem. Phys.* **1979**, *70*, 4963.

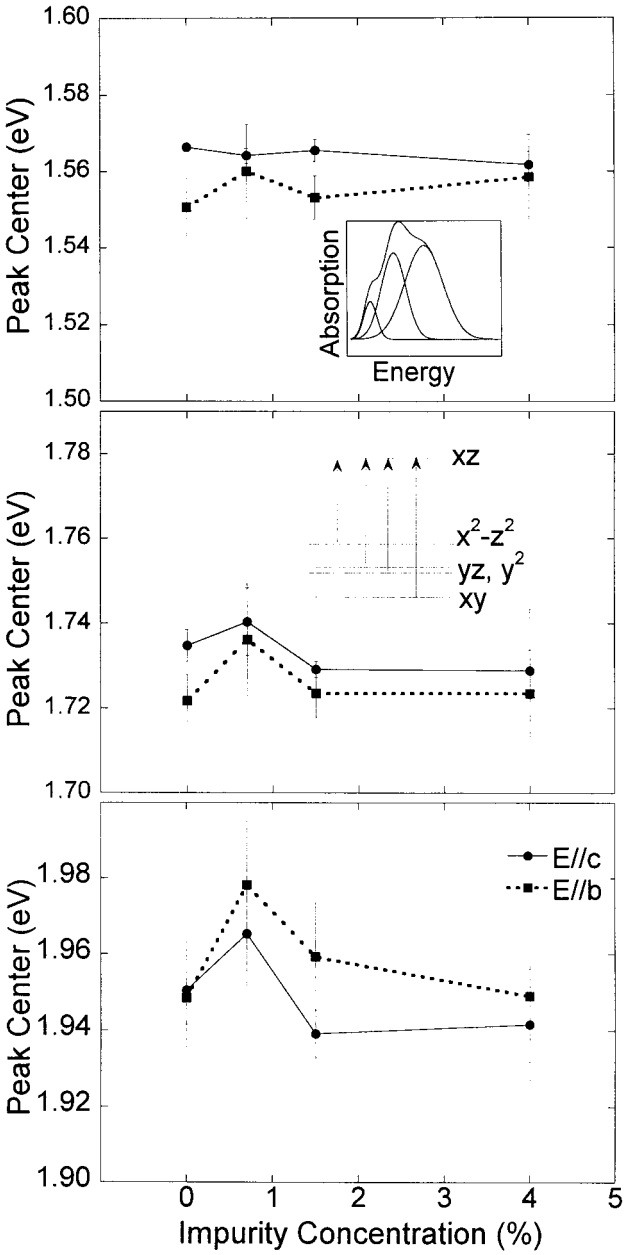

Figure 4. Center positions of the model oscillators fit to the phonon-assisted d-band vs Zn impurity concentration. Upper panel inset: example of the d-band fitting with three oscillators. Middle panel inset: energy level scheme that provides the basis for the fitting. Energy differences (indicated by arrows) are calculated to be 1.73, 1.88, 1.89, and 1.94, respectively. Solid and dashed lines guide the eye and correspond to E||*c* and E||*b* polarizations, respectively. The error bars are deduced from the statistical analysis of the four fitting runs with slightly different fitting procedures.

O $2p_x$ and O $2p_y$ orbital contributions can be calculated separately.

On the basis of the PDOS curves shown in Figure 2, we now discuss the nature of the electronic transitions responsible for both the anisotropic absorption edge and the dual slope along *b* in $CuGeO_3$. The relevant excitations are clearly charge transfer in character. The sharp absorption edge in the *E*||*c* polarization can be assigned to O $2p_x$, $2p_y \rightarrow$ singly filled Cu 3d excitations. Because the O $2p_x$, $2p_y$ maxima in the densities of state nearly coincide and the overall shapes are similar and feature-

less, no peculiarities in the absorption edge are expected or observed. The *b* direction is different. Here, the edge can be ascribed to O $2p_z \rightarrow$ singly filled Cu 3d transitions. Note that the PDOS of O $2p_z$ has two maxima, largely because adjacent O $2p_z$ orbitals, being aligned along the chain direction, overlap and form a one-dimensional band. The joint densities of state for the optical transition should reflect this double maxima structure, and the optical absorption is expected to display two slopes. That the O $2p_z$ states appear at lower energy than the $2p_x$ or $2p_y$ states explains the higher energy absorption onset along *b*. Thus, both the anisotropy between the *b* and *c* axis spectra and the dual slopes on the edge of the optical charge-transfer gap along *b* follow directly from the excitations involved and the PDOS shapes.

The above assignments of the anisotropic charge-transfer excitations are consistent with a site symmetry analysis of an isolated CuO_6 octahedron. The $O_{ap}-Cu-O_{ap}$ axis is not perpendicular to the basal plane of the CuO_6 octahedron, and the CuO_6 octahedron has a mirror plane of symmetry perpendicular to the CuO_4 chain direction, a rotation axis in the basal plane, and an inversion center. Thus, the site symmetry of each CuO_6 octahedron is C_{2h}. Analysis of the transition dipole moment involving the singly filled 3d level of a CuO_6 octahedron shows that for the *z* polarization ($E \| c$), the charge-transfer excitation involves the O $2p_x$ and $2p_y$ orbitals of all of the axial and equatorial oxygen atoms of the CuO_6 octahedron and the O $2p_z$ orbitals of only the equatorial oxygen atoms. For the *x* or *y* polarization ($E \perp c$), the charge-transfer excitation involves the O $2p_z$ orbitals of all of the axial and equatorial oxygen atoms of the CuO_6 octahedron and the O $2p_x$ and $2p_y$ orbitals of only the equatorial oxygen atoms. Whereas transition energies are fixed by the orbitals involved, group theory tells us nothing about intensities. Nevertheless, it is reasonable to assume that the transition dipole moment will be large when all of the axial and equatorial oxygen atoms of the CuO_6 octahedron are involved in the excitation, because the number of the oxygen p-orbital states participating in the excitation will be large in this case. This supports the assignments given above.

B. Doping Dependence of the Electronic Transitions in $CuGeO_3$. Figure 3 compares the absorption spectra of pure, 4% Zn-doped, and 0.7% Si-doped $CuGeO_3$ in both *b* and *c* polarizations. As expected, the two types of impurities influence the spectra in fundamentally different ways. Whereas heavy Zn doping has a limited impact on the optical spectra, the Si-doped crystals exhibit notable smearing of the absorption edge. Below, we divide our discussion into two parts: the doping dependence of the electronic gap regime and the effect of impurities on the phonon-assisted d band for the $Cu_{1-x}Zn_xGe_{1-y}Si_yO_3$ system.

1. Doping Effects Near the Gap Edge. The Si-substituted sample displays different behavior from that of pure $CuGeO_3$ in the energy range near the 3 eV charge-transfer gap excitations (Figure 3). Instead of the abrupt edge in the $E \| c$ polarization and the aforementioned dual-slope edge in the $E \| b$ polarization that are characteristic of the pure material, the leading edge of the gap is smeared in both directions. Note that only 0.7% Si substitution is required to induce this smearing.

In contrast, no observable changes are found in the shape of the absorption edge in Zn-doped $CuGeO_3$. This is because the CuO_6 octahedra and overall lattice are undistorted by the substitution, as discussed below. It is worth reemphasizing that the spectrum shown in Figure 3 corresponds to the most heavily substituted $Cu_{1-x}Zn_xGeO_3$ crystal, and even the high-impurity concentration (4%) does not noticeably change the shape of the charge-transfer edge in either polarization. Thus, we conclude that Si substitution, which modulates the transverse interactions, is much more effective than Zn in altering the charge-transfer properties of $CuGeO_3$.

The behavior described above may originate from different structural changes introduced into the lattice by the two different types of impurities. Doping with Si causes essential modifications in the crystal structure, contributing to changes in all three lattice parameters and the overall unit cell volume.[19] It is reasonable to expect that, at low doping levels, these changes are small and fairly localized. Time-of-flight neutron powder diffraction experiments[36] show that silicon−oxygen bonds in the Si-doped material become shorter as compared to germanium−oxygen bonds in the pure material. At the same time, the bond between Cu and O in the basal plane does not depend on the Si content, and the $Cu-O_{ap}$ bond length increases slightly. Thus, Si substitution causes random deformations in the chain of GeO_4 tetrahedra and related randomly distributed elongations of CuO_6 octahedra. We suggest that light Si impurity substitution leads to weak local distortions of the lattice, and irregularities in the deformation potential profile reveal themselves in the smearing of the absorption edge in $CuGe_{0.993}Si_{0.007}O_3$. Essentially, this is a structurally induced change in the electronic properties.[37]

In contrast, Zn substitution does not alter the crystal lattice parameters.[1] This is because the ionic radius of Zn is nearly identical with that of Cu (0.75 and 0.73 Å, respectively) and both are divalent. Thus, doping with Zn should not introduce substantial mechanical strain nor should it modify the electrostatic forces in the CuO_6 (ZnO_6) octahedron. The dramatic consequences of the Zn doping on the SP phase diagram have a different origin because Zn has $S = 0$; Zn substitution on the Cu site causes fragmentation of the $S = {}^1/_2$ chains.[1,2,4−6]

2. Influence of Doping on the d Band. In accordance with the complex shape of the d band near 1.7 eV and expected crystal field effect on the Cu^{2+} ion, we fit the phonon-assisted d band with three separate oscillators, as shown in the inset to the upper panel of Figure 4. These three oscillators are intended to mimic the four transitions depicted in the middle panel of Figure 4, predicted by extended Hückel molecular orbital calculations for an isolated CuO_6 octahedron.[39] Two of the four transitions are nearly degenerate and therefore would be indistinguishable in the spectral

(36) Braden, M.; Buchner, B.; Klotz, S.; Marshall, W. G.; Behruzi, M.; Heger, G. *Phys. Rev. B* **1999**, *60*, 9616.

(37) Oxygen contamination in Si-doped crystals is cited in some studies,[19,36] but we find no need to resort to such an explanation for these results.

(38) Ammeter, J.; Bürgi, H.-B.; Thibeault, J.; Hoffmann, R. *J. Am. Chem. Soc.* **1978**, *100*, 3686.

response. The goal of our fitting procedure was to assess the doping dependence of the d-band parameters and understand how such doping dependence contributes to the color properties of $CuGeO_3$-based materials.

To analyze the influence of doping on the d-band behavior, we have plotted the center positions of the three model oscillators vs Zn impurity concentration for the two polarizations of interest (Figure 4). All three bands exhibit very weak, if any, impurity concentration dependence, and within the error bars, we find that the d-band excitations are independent of Zn doping.[40] Behavior of this type suggests that the first nearest neighbors (O ions in the basal plane) are primarily responsible for the local symmetry of the crystal field at the Cu site and, thus, for the Cu^{2+} d-band splitting. The nearest metal centers, Cu^{2+} or substituted Zn ions, apparently play a minimal role in shaping the phonon-assisted d band and do not contribute to the color properties of the material. This result is in good agreement with the localized nature of d−d transitions in other transition-metal complexes.

In addition, we have modeled the cluster of excitations near 1.7 eV in the 0.7% Si-substituted sample (not shown) using similar techniques. The parameters of the three constituent bands are unchanged within the resolution of our fits. Thus, distortions brought about by the SiO_4 tetrahedra, which cause the aforementioned changes in the absorption edge region near 3 eV, do not manifest themselves in the d-band regime. This suggests that either the d−d transitions in the affected octahedra are unmodified (or insignificant) compared with the response of the unaffected octahedra or that the phonon-assisted d−d transitions become ineffective in distorted CuO_6 octahedra.

(39) The choice of the coordinate system determines the labeling of the crystal field split d-block orbitals. For instance, note that our calculated d-block energy level ordering differs from the one proposed in ref 15.

(40) The lack of doping dependence in the phonon-assisted d-band fit parameters suggests that these excitations are mechanistically unrelated to the 1.47 eV zero phonon line, even though the two structures are fortuitously near each other in energy.[41]

(41) Long, V. C.; Rudko, G. Y.; Zhu, Z. T.; Musfeldt, J. L.; Wei, X.; Schmeidel, T.; Revcolevschi, A.; Dhalenne, G., unpublished results.

IV. Conclusion

We report polarized optical transmission measurements of both pristine and doped $CuGeO_3$. Our electronic structure calculations suggest that, with the *z* axis taken along the CuO_4 chain direction, the anisotropic absorption edge of $CuGeO_3$ can be attributed to the following charge-transfer transitions: O $2p_x$, $2p_y \rightarrow$ singly filled Cu 3d (*E*||*c*) and O $2p_z \rightarrow$ singly filled Cu 3d (*E*||*b*). Because the O 2 p_z state has two local maxima, two slopes are observed in the absorption edge in the *E*||*b* spectra. Doping with Si causes an essential smearing of the absorption edge in both polarizations, which we assign as a structurally induced change in the electronic properties.

Acknowledgment. Financial support for work at SUNY Binghamton from the Materials Science Division, Basic Energy Sciences at the U.S. Department of Energy (Grant DE-FG0299ER45741), is gratefully acknowledged. Work at North Carolina State University was supported by the Office of Basic Energy Sciences, Division of Material Sciences, U.S. Department of Energy, under Grant DE-FG05-86ER45259.

CM000703F